Chemistry & Biology, Vol. 10, 351–359, April, 2003, ©2003 Elsevier Science Ltd. All rights reserved. DOI 10.1016/S1074-5521(03)00077-2

Rational Engineering of a DNA Glycosylase Specific for an Unnatural Cytosine:Pyrene Base Pair

Keehwan Kwon, Yu Lin Jiang, and James T. Stivers*
Department of Pharmacology and Molecular Sciences
The Johns Hopkins University School of Medicine
725 North Wolfe Street
Baltimore, Maryland 21205

Summary

A novel site-specific cytosine DNA glycosylase has been rationally engineered from the active site scaffold of the DNA repair enzyme uracil DNA glycosylase (UDG). UDG, which operates by a nucleotide flipping mechanism, was first converted into a sequence nonspecific cytosine DNA glycosylase (CDG) by altering the base-specific hydrogen bond donor-acceptor groups in the active site. A second mutation that renders UDG defective in nucleotide flipping was then introduced, and the double mutant was rescued using a substrate with a "preflipped" cytosine base. Substrate-assisted flipping was engineered by incorporation of an unnatural pyrene nucleotide wedge (Y) into the DNA strand opposite to the target cytosine. This new enzyme, CYDG, can be used to target cleavage of specific cytosine residues in the context of a C/Y base pair in any DNA fragment.

Introduction

DNA glycosylases initiate the process of base excision repair (BER) by cleaving the *N*-glycosidic bond of damaged or mismatched bases in DNA [1]. One of the most frequent base modifications is the conversion of cytosine to uracil by hydrolytic deamination [2]. This lesion may directly disrupt the interactions of proteins with their specific sites in DNA [3, 4], and if replicated, results in C/G → T/A transition mutations. Thus, a highly efficient uracil excision repair pathway has evolved, which begins with enzyme-induced flipping of the deoxyuridine nucleotide from the DNA duplex, followed by cleavage of the glycosidic bond by the enzyme uracil DNA glycosylase (UDG) [5]. UDG has evolved under tremendous selection pressure not to excise normal bases in DNA, because such events lead to toxic abasic lesions [6]. Indeed, it has been impossible to detect the removal of any other naturally occurring base by UDG, which sets a lower limit on its specificity of $\geq 10^6$ $[(k_{cat}/K_m)^U/(k_{cat}/K_m)^{A,T,C,\text{ or }G}]$ [7]. This remarkable specificity of UDG for uracil results from a number of factors including steric selection [8, 9], hydrogen bonding [10–13], and more importantly an induced fit conformational step that serves as a secure gateway to the powerful catalytic machinery of UDG [14, 15].

Steric effects play a major role in selecting against other bases entering the active site. The small size of the uracil binding pocket easily prevents access of normal purine bases to the active site, and the conserved active site residue, Tyr66 of *Escherichia coli* UDG (*e*UDG), which corresponds to Tyr147 of human UDG (*h*UDG), forms a rigid wall that prevents thymine from entering the pocket [8, 9, 16]. Indeed, UDG activity is very sensitive to substitutions at the 5 or 6 positions of the pyrimidine ring, and DNA analogs such as 5-bromodeoxyuridine are not substrates for the enzyme [17]. Consistent with the proposed steric role for this tyrosine residue in generating specificity, the Y147A mutant of *h*UDG removes uracil as well as thymine bases from DNA [8].

Hydrogen bonding is used to form energetically favorable interactions that are highly specific for the uracil base (Figure 1A). Selection against cytosine involves the side chain amide of Asn123 that is rigidly positioned to donate a hydrogen bond to uracil O4 and accept a hydrogen bond from H3 [13], which is the opposite pattern required to recognize cytosine (Figure 1A). Perhaps more important is the observation that the N123G mutant is severly damaged with respect to an induced fit conformational change that allows wtUDG to clamp around the uracil base [15]. It would therefore appear that the O4 and H3 hydrogen bonding interactions are key to achieving the catalytically productive Michaelis complex.

The induced fit conformational change in UDG links the steps of uracil flipping and glycosidic bond cleavage and is the single most important determinant of specificity [14, 15]. UDG is a prototypic base flipping enzyme that extrudes the damaged uracil base from the DNA duplex prior to cleavage of the glycosidic bond [7, 9, 14, 15, 18]. In general, induced fit is a powerful mechanism for generating specificity when it leads to catalytic interactions that are available for one preferred substrate, such as deoxyuridine, but not other potential substrates. Leu191 of *e*UDG has been strongly implicated in the induced fit specificity mechanism of UDG by pushing the cognate uracil base from the DNA duplex, and by increasing its lifetime in the active site by sterically blocking its exit [19]. Like the N123G mutant, L191A is severely crippled with respect to the conformational change that is required for catalysis [14, 15], showing that the mechanical role of Leu191 is tightly coupled to the formation of the active enzyme-substrate complex.

Based on this information, we wondered whether these elements of specificity could be manipulated to transform UDG into a site-specific cytosine DNA glycosylase. Previous mutagenesis studies have shown that the N204D mutation of *h*UDG, and the corresponding N123D mutation for *e*UDG, transformed these enzymes into cytosine DNA glycosylases (CDG), while retaining a good portion of the original UDG activity (Figure 1A) [8, 20]. The structural basis for this new CDG activity presumably arises from the complementary hydrogen bonds between the newborn aspartic acid side chain and the exocyclic and endocyclic nitrogen atoms on the cytosine base (Figure 1A). However, neither of these

*Correspondence: jstivers@jhmi.edu

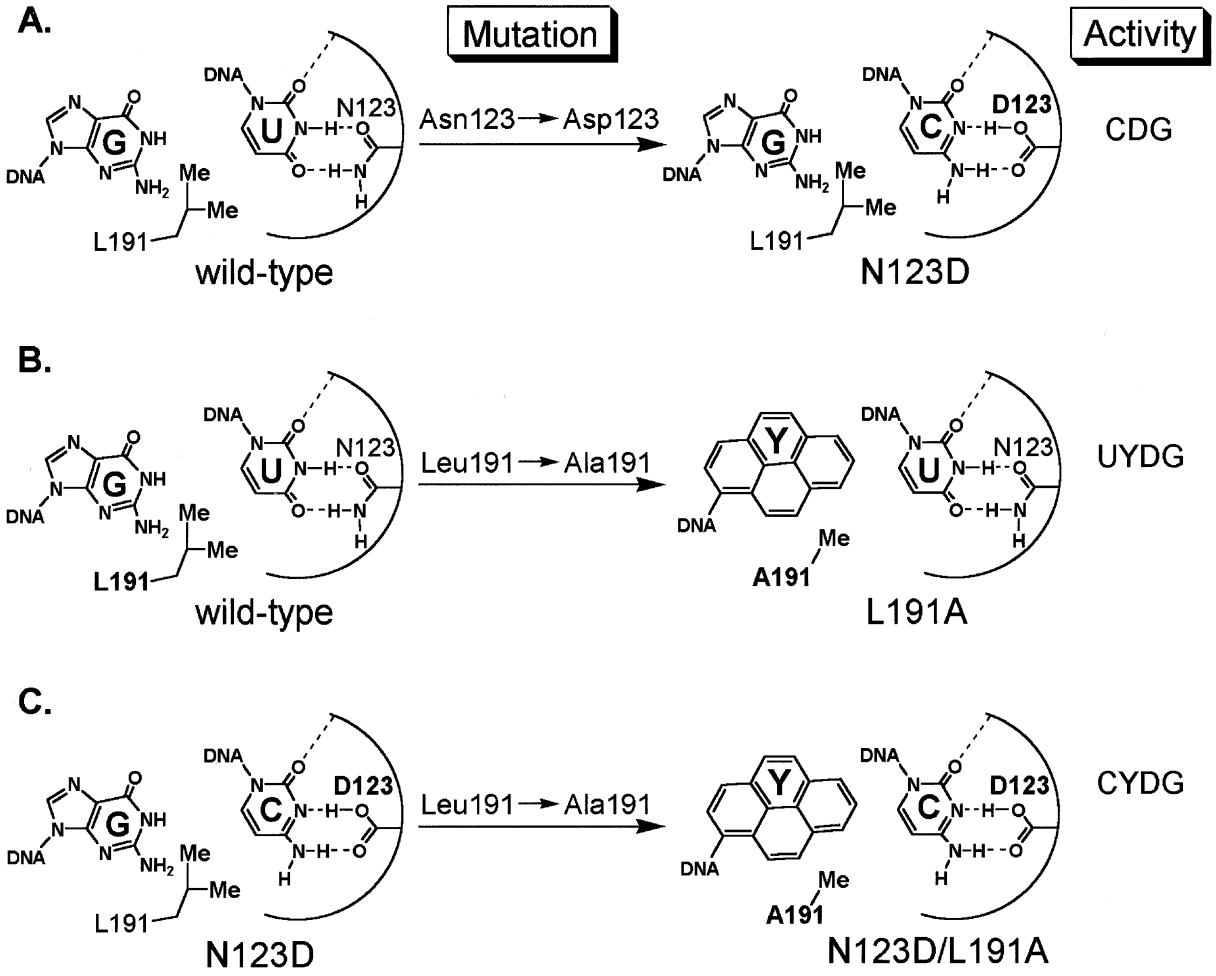

Figure 1. Engineering a New Base-Specific Glycosylase Activity of UDG

(A) Mutation of Asn123 to Asp generates an enzyme that exhibits specificity for cytosine bases, as previously demonstrated for *h*UDG [8].

(B) The low catalytic activity of the L191A UDG base flipping mutant can be fully rescued by incorporation of a pyrene nucleotide wedge into the DNA strand opposite to the position of uracil.

(C) A new sequence-specific (C/Y) DNA glycosylase activity (CYDG) was designed by combining the two mutations, N123D and L191A.

previous reports removed the aspartic acid side chain to test the requirement for these hydrogen bonds in the new CDG activity. More recently, it has been shown that the L191A flipping-deficient mutant of *e*UDG can be converted into a glycosylase that has enhanced specificity for unnatural uracil/pyrene base pairs (Figure 1B) [14, 15, 19]. The physical basis for this specificity arises from two effects: the L191A mutational effect, which greatly hinders active base flipping by removing the wedge group, and substrate rescue by the bulky pyrene nucleotide (Y), which acts as a surrogate wedge for Leu191. In other words, the pyrene wedge preorganizes the uracil base in an extrahelical conformation, allowing recognition and catalysis to occur in the absence of enzyme-induced flipping [14, 15, 19].

In this report, we demonstrate that these two specificity mechanisms can be combined to generate a new DNA glycosylase that is extraordinarily specific for a C/Y base pair (Figure 1C). The double mutant, N123D:L191A, locates and cleaves cytosine in a C/Y base pair, but does not cleave cytosine in a normal C/G base pair. This specificity should allow targeted cleavage of any cytosine residue in a given gene fragment by simply hybridizing a complementary DNA strand that contains an unnatural pyrene nucleotide in the correct position.

Results

Constructing and Expressing the D123N:L191A Double Mutant

In general, attempts at engineering a DNA glycosylase to recognize a normal base will be met with adversity because such enzymes will remove normal bases in the genome and will be highly toxic to the organism that harbors the gene. Indeed, the initial mutagenesis study where *h*UDG was converted into a cytosine DNA glycosylase (N204D) reported that this gene construct was highly toxic to bacteria, and that the expression constructs were not stable unless a recombination-deficient *rec*A$^-$ *Escherichia coli* strain was utilized [8]. For the

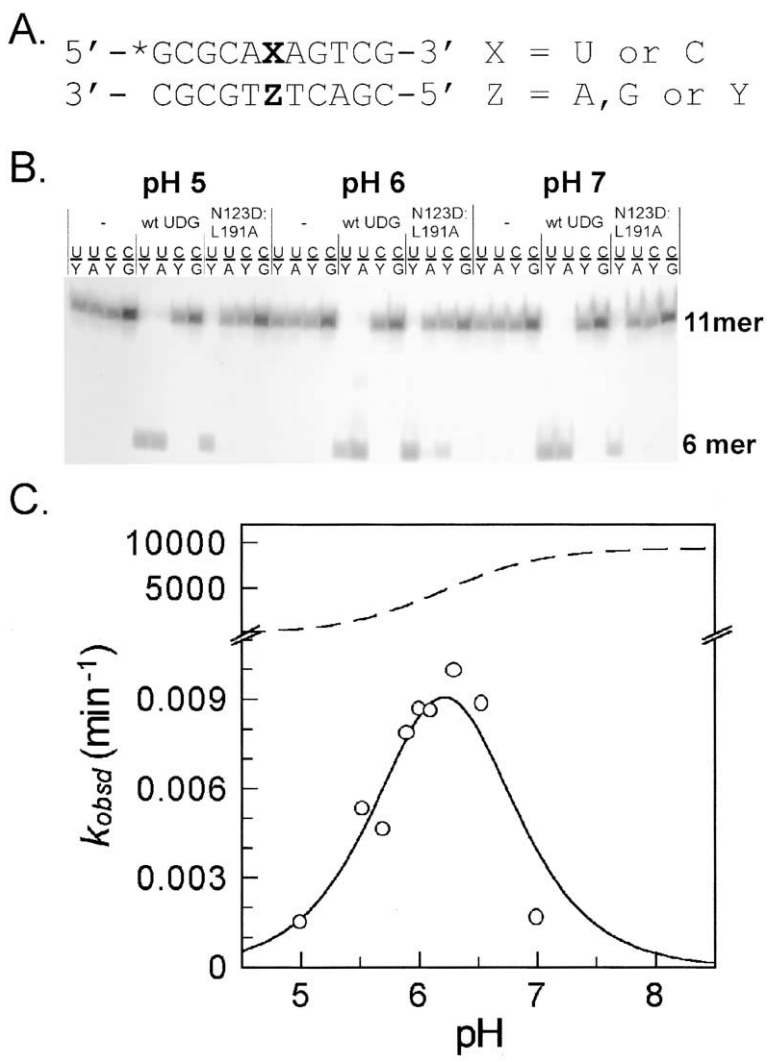

Figure 2. pH Dependence of CYDG Activity

(A) The middle base of the 11-mer DNA substrate was varied to generate U/Y, U/A, C/Y, or C/G base pairs. The 5′-end of the top strand was labeled with ^{32}P (*).

(B) The pH dependence of the CYDG activity was studied using four ^{32}P-labeled DNA substrates, C/Y, C/G, U/Y, and U/A. The 11-mer substrate and 6-mer product were resolved on a 20% denaturing polyacrylamide gel. The concentrations of wtUDG and CYDG were 10 nM and 100 nM, respectively, and the DNA substrate concentrations were 250 nM.

(C) The pH dependence of k_{obsd} for CYDG using the C/Y substrate (open circles). For comparison, the previously determined pH dependence of k_{cat} for wtUDG is shown as a dashed line [21].

analogous eUDG mutation (N123D), we were unable to obtain transformants under any conditions (not shown), suggesting that this mutation was even more toxic than reported for the human enzyme.

One general strategy to overcome this severe toxicity problem is to generate the toxic N123D mutation in a background of the L191A mutation, which prevents base flipping of normal bases and therefore cleavage of these bases in vivo. This approach allowed isolation of stable transformants of the N123D:L191A mutant, and the corresponding enzyme was easily overexpressed and purified. The expected cytosine/pyrene DNA glycosylase (CYDG) activity could then be characterized in vitro using a DNA substrate containing a cytosine/pyrene base pair (Figure 1C). Of course, an alternative strategy would be to use an in vitro transcription and translation system to express the N123D enzyme [20]. However, the N123D single mutant does not exhibit any sequence specificity, as previously reported for the analogous mutation in human UDG [8].

pH Dependence of CYDG Activity

As a first step in characterizing this new enzyme, we determined the pH dependence of its activity against four potential substrates that contained U/Y, U/A, C/Y, and C/G base pairs (Figure 2A). The 5′-end of the DNA strand containing the target base was labeled with ^{32}P, and after reaction with CYDG for 30 min the substrates were treated with 1 M piperidine to cleave the DNA backbone at the abasic site of the product DNA. The 11-mer substrates and 6-mer products were then resolved by 20% denaturing PAGE (Figure 2B).

CYDG shows a pronounced bell-shaped pH-rate profile with a maximal rate occurring in a narrow pH range centered at pH 6.2, indicating that a protonated and unprotonated group on the enzyme or substrate is required for activity against the C/Y substrate (open circles, Figure 2C). This pH dependence differs significantly from wtUDG [21], which only requires a *single* unprotonated group for activity under k_{cat} conditions (dashed line, Figure 2C). In the pH range 5 to 8, CYDG showed activity against the C/Y, U/Y, and U/A substrates. For all of these substrates, k_{cat} diminished by almost 10-fold between pH 6.3 and 8, suggesting a common requirement for a protonated group on CYDG for maximal activity. In contrast, wtUDG showed no activity against the cytosine-containing substrates, but did efficiently remove uracil in the context of either a U/Y or

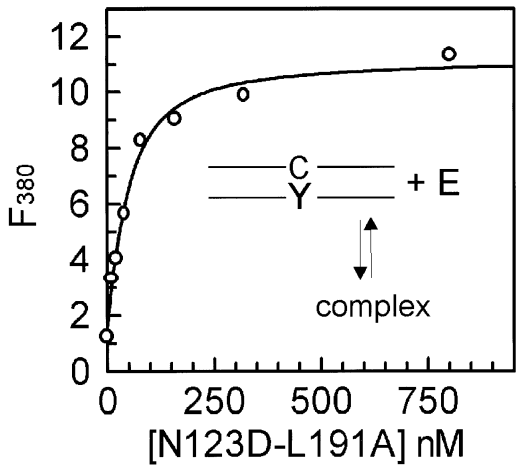

Figure 3. Binding Affinity of CYDG for a C/Y Base Pair

The equilibrium titration was performed with 40 nM DNA substrate in a buffer containing 10 mM sodium phosphate, 25 mM NaCl, and 2.5 mM $MgCl_2$ at pH 6.0. The intensity of fluorescence was monitored at 380 nm with excitation at 350 nm. Each titration point represents the independent addition of a given enzyme concentration to a fresh sample of DNA to prevent substrate cleavage over the course of a complete titration. The solid line is the nonlinear least-squares best fit to equation 4. The equilibrium dissociation constant is 28 ± 8 nM from this analysis.

U/A base pair at all pH values tested. *Importantly, CYDG did not excise cytosine in the context of a C/G base pair* (Figure 2)*, and thus, with respect to the four normal DNA bases, exhibits specific CYDG activity* (see also Figure 4A). The apparent pK_{a1} and pK_{a2} values for CYDG were obtained using the standard equation describing a bell-shaped pH profile (equation 3, see Experimental Procedures). The optimum pH of 6.2 ± 0.1 was obtained from the average of the apparent values, pK_{a1} = 6.1 ± 0.1 and pK_{a2} = 6.3 ± 0.1. These apparent pK_a values will differ from the true pK_a values because pK_{a1} and pK_{a2} are very close to one another [22].

DNA Binding Specificity of CYDG

To examine the binding specificity of CYDG at its optimal pH of 6.2, we followed the increase in pyrene fluorescence of an 11 base pair substrate DNA that contained a C/Y base pair (Figure 3). During these measurements, less than 0.2% of the C/Y substrate was cleaved due to the short measurement times (see Experimental Procedures). Surprisingly, these results showed that CYDG binds to the C/Y 11-mer as tightly as wtUDG or the L191A mutant binds to U/Y DNA (K_D = 28 ± 8 nM) [19]. These binding measurements strongly suggest that CYDG is interacting specifically with the C/Y base pair, and likely employs the hydrogen bonding interactions indicated in Figure 1C. In support of this conclusion, the N123G mutant does not bind tightly to U/Y or U/A DNA ($K_D \sim 5$ μM) [14, 15], and it is unable to excise cytosine from a C/Y base pair (see below). Thus, the thermodynamic measurements show that the Asp123 side chain is required for specific binding to C/Y base pairs.

Catalytic Specificity of CYDG

At the optimum pH of 6.2 ± 0.1, the substrate specificity of CYDG was studied with seven DNA substrates that contained a variety of base pairs. This analysis indicated that CYDG selectively excises cytosine from a C/Y pair, and does not cleave the glycosidic bond of adenine, guanine, and thymine even when these bases were presented in the context of an N/Y base pair (N = A, G, or T) (Figure 4A). Despite this high selectivity for the C/Y base pair, CYDG still possesses strong uracil DNA glycosylase activity (Figure 4A). The residual UDG activity at pH 6.3 is about 10-fold *faster* than that of the N123G mutant, which shows no detectable CDG or CYDG activity (Table 1). However, the residual UDG activity of CYDG at pH 8 is 30-fold *less than* N123G, presumably because Asp123 is anionic, resulting in electrostatic destabilization of the anionic leaving group (see Discussion). Thus, the Asp123 side chain provides specificity for cytosine over uracil only at pH values near 6.2 where Asp123 is in the appropriate protonation state.

In order to understand the new CYDG activity, detailed kinetic studies were performed using the C/Y duplex at pH 6.3 (Figure 4B). CYDG showed the expected steady state kinetic behavior with the C/Y, U/A, and U/Y substrates, with linear initial rates, and hyperbolic substrate saturation curves (Figures 4B and 4C). CYDG exhibits a strong C/Y DNA glycosylase activity with a k_{cat}/K_m of 8×10^5 M^{-1} min^{-1}, and it is 300- and 10^5-fold less active than wtUDG against the U/Y and U/A substrates, respectively. The catalytic specificities (S) of CYDG and wtUDG for the C/Y and U/Y substrates may be obtained from the ratio $S = (k_{cat}/K_m)^{C/Y}/(k_{cat}/K_m)^{U/Y}$ for each enzyme. This ratio is at least 100,000-fold greater for CYDG than for wild-type UDG, where $S \leq 4.5 \times 10^{-8}$. Therefore, the combined mutatagenesis and substrate rescue approach has dramatically altered the substrate specificity of UDG. Impressively, the excision of cytosine from a C/G base pair by CYDG could not be detected. Based on the detection limits of the gel-based ^{32}P assay, we estimate that CYDG has a ≥ 2600-fold preference for cleavage of cytosine from a C/Y base pair as compared to a C/G base pair. Whether this specificity is sufficient to recognize C/Y in any given DNA fragment remains to be established.

Discussion

Studies of Lethal DNA Repair Mutants Using a Substrate Rescue Strategy

The pyrene rescue strategy is quite valuable in the study of highly toxic UDG mutants. In the study described here, the *e*UDG mutant, N123D:L191A, was successfully overexpressed and purified, while N123D was completely inaccessible because of its toxicity to bacterial cells. Although the corresponding N204D mutation in *h*UDG has been reported [8], sufficient quantities of this enzyme were not attainable from bacterial expression systems for structural or mechanistic studies. In contrast, CYDG can be obtained in copious quantities, and exhibits nearly the same k_{cat} as the human N204D mutant [8]. We have also used this strategy to successfully overexpress the Y66A:L191A mutant, which would be expected to show specific TYDG activity. As expected, this enzyme does show a high specificity for cleavage of thymine in the context of a pyrene base pair, but we

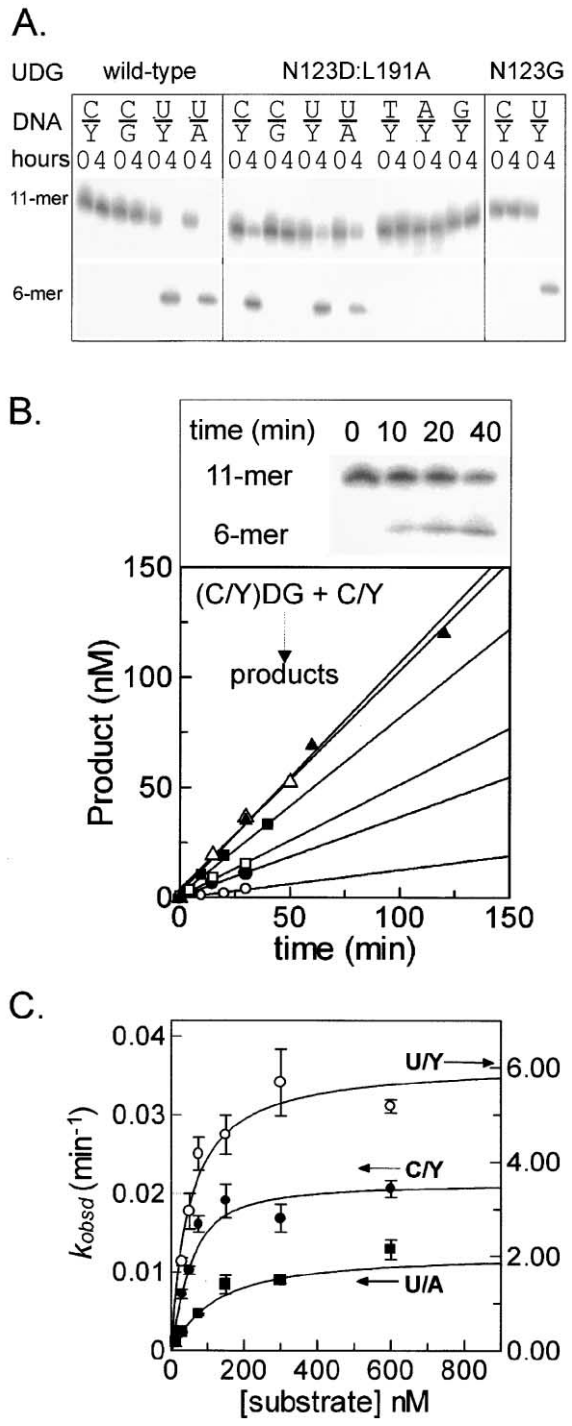

Figure 4. Base Specificity and Kinetic Measurements

(A) Base specificity of wtUDG, CYDG, and the N123G mutant was examined using the ^{32}P-labeled 11-mer DNA substrates as indicated. The cleavage reactions were performed in buffer A for 4 hr at 25°C.

(B) Initial rate measurements for CYDG using the C/Y 11-mer. The upper panel is a representative cleavage reaction as a function of time. The lower panel is a plot of product 6-mer as a function of time for various concentrations of substrate DNA [15 nM (open circles), 30 nM (closed circles), 50 nM (open squares), 75 nM (closed squares), 150 nM (open triangles), and 600 nM (closed triangles)]. The solid lines are linear least-squares best fits to the data.

(C) Kinetic behavior of CYDG with U/Y (open circles), C/Y (closed circles), and U/A (closed squares) substrates. The solid lines are the nonlinear least-squares best fits to the data using equation 2. The *y* axis scale for the U/Y substrate is shown on the right, and that for the U/A and C/Y substrates is shown on the left.

did not completely characterize this enzyme because its activity was only 1/100 of CYDG (not shown). Nevertheless, the specificity of TYDG is significant because we were unable to detect any cleavage of thymine in the context of a T/A base pair. Based on these results, the mutagenesis-pyrene rescue approach appears to be generally applicable for the generation of N/Y-specific glycosylases.

Catalytic Power and Specificity of CYDG

CYDG is a powerful cytosine DNA glycosylase with exquisite specificity. The nonenzymatic hydrolysis rate for deoxycytodine at 25°C ($k_{obsd} = 3.5 \times 10^{-9}$ s^{-1}) may be calculated from the temperature dependence studies of Shapiro and Danzig [23]. This slow rate is 114,000-fold slower than k_{cat} for CYDG, and indicates that CYDG lowers the activation barrier by 7 kcal/mol ($= -RT \ln k_{cat}/k_{obsd}$) as compared to the nonenzymatic reaction. The rate enhancement of CYDG is considerably less than the 10^{12}-fold catalytic power of UDG, and is 10^4-fold less than another pyrimidine-specific glycosylase, thymine DNA glycosylase [24, 25]. Nevertheless, the CYDG activity compares favorably with many other naturally occurring DNA glycosylases. CYDG provides a larger rate enhancement than several glycosylases that act on alkylated purine bases, such as human alkyl adenine DNA glycosylase (AAG) [26, 27], and the observed rate for excision of cytosine by CYDG (0.024 min^{-1}) is similar to the maximal rate of AAG with DNA containing an ethenoadenine base (0.075 min^{-1}) [26]. To our knowledge, a site-specific cytosine DNA glycosylase activity does not exist in nature, and the success of this engineering approach relies heavily on the tremendous catalytic power of the native UDG active site scaffold.

How specific is CYDG? Our primary goal was to generate an enzyme that would specifically recognize cytosine in the context of a C/Y base pair, and would not excise the other four naturally occurring DNA bases in normal Watson-Crick base pairs. By this criteria, CYDG performs exceptionally well. Based on the detection limits of our kinetic assays, we can conclude that CYDG excises cytosine in the context of a C/Y base pair *at least* 2600-fold more efficiently than a C/G base pair. Its discrimination against binding and cleavage of other bases is likely much higher than this lower limit for cytosine, given that the nature of the UDG active site naturally deters binding of T, A, and G (see above). However, CYDG is less efficient in discriminating against uracil, and shows only a 6-fold discrimination against U/A as compared to C/Y, and the U/Y substrate is actually preferred over C/Y by a factor of 100-fold at pH 6.3 (Table 1). This residual UDG activity is not unexpected in light of previous studies showing that UDG active site mutations never fully ablate enzyme activity [14–16, 21]. As described further below, part of the inability of CYDG to discriminate against uracil is that the protonated Asp123

Table 1. Kinetic Parameters for Wild-Type and UDG Mutants

Enzyme	Substrate	k_{cat} (min^{-1})	K_m (μM)	k_{cat}/K_m ($\mu M^{-1}min^{-1}$)
wild-type	AUA/TAT	318 ± 36	0.020 ± 0.004	15,900 ± 3,700
	AUA/TYT	696 ± 30	0.018 ± 0.003	38,700 ± 6,700
N123D-L191A	ACA/TYT	0.024 ± 0.003	0.03 ± 0.01	0.80 ± 0.28
	AUA/TAT	0.012 ± 0.001	0.09 ± 0.01	0.133 ± 0.019
	AUA/TYT	6.12 ± 0.48	0.05 ± 0.01	122 ± 26
N123G[a]	AUA/TAT	2.3 ± 0.2	2.1 ± 0.4	1.1 ± 0.2
	AUA/TYT	50 ± 5	1.44 ± 0.46	34.7 ± 0.3

side chain is fully complementary to the hydrogen bond donor-acceptor groups on both the uracil and cytosine bases (Figure 5), resulting in strong binding affinity for both (compare the low K_m values of wtUDG and CYDG with that of N123G in Table 1).

Potential Mechanisms for CYDG

The pH dependence of the CYDG activity, and its residual UDG activity, suggest possible chemical mechanisms for its action (Figure 5). The bell-shaped pH-rate profile suggests that two essential groups on CYDG are

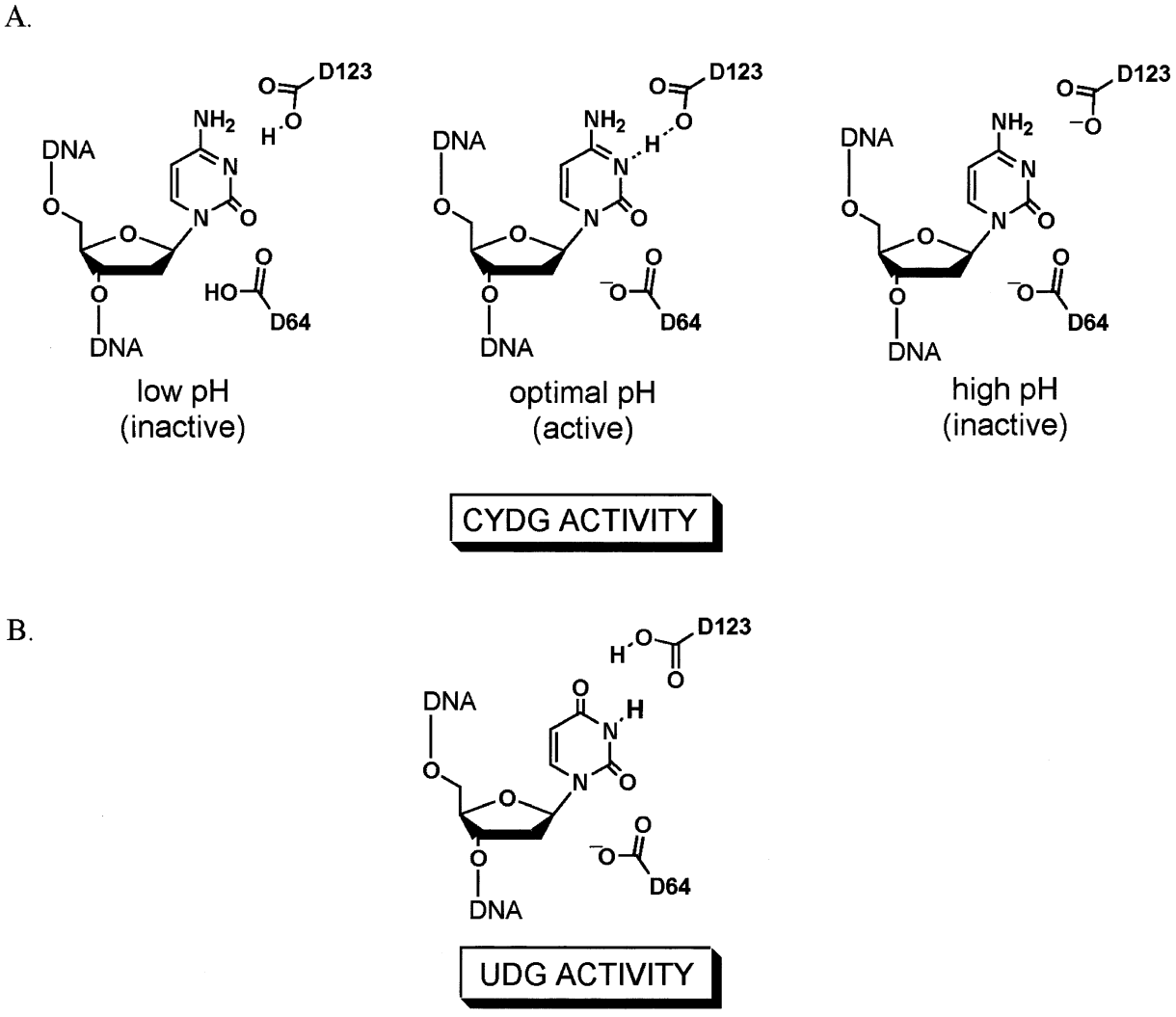

Figure 5. Possible Chemical Mechanisms for CYDG

(A) The pH dependence of CYDG suggests the requirement for a base and acid group in the action of the enzyme (Figure 2C). The base group is likely Asp64 (pK_a = 6.2) based on previous studies with wtUDG, which strongly implicate this group in the stabilization of a cationic sugar during glycosidic bond hydrolysis [21]. The acid group is likely Asp123, which could hydrogen bond to the exocyclic and endocyclic amino groups of the cytosine base in the ground state and could transfer a proton to cytosine N3 in the transition state.

(B) The residual UDG activity of CYDG may be explained by tautomerization of Asp123, which permits correct hydrogen bonding to the uracil base analogous to the native Asn123 (Figure 1A).

required for activity. One group must be in the unprotonated state for activity, which accounts for the ascending limb as the pH is increased between 5 and 6, and the second group must be in a protonated state, which accounts for the decrease in activity as the pH is increased above 6 (Figure 2). It is likely that only a small fraction of CYDG is in the correct protonation state even at the optimal pH of 6.2, because the apparent pK_a values of these groups are extremely close to each other, preventing the optimal protonation state from being fully achieved at any pH value. Based on previous knowledge of the pH dependence of wtUDG [28], it is likely that the ascending limb represents deprotonation of Asp64 (pK_a = 6.2) [21], which is required in the anionic state to stabilize the positive charge that develops on the sugar ring during catalysis [29–31]. The relatively high pK_a for Asp64 in the ES complex is likely due to the electrostatic environment provided by the anionic phosphodiester groups of the DNA. The descending limb, which is not observed for wtUDG [21], or the N123G mutant (not shown), is likely due to deprotonation of Asp123, which also suggests a high pK_a for this group (Figure 5). A protonated Asp123 could serve a beneficial role by hydrogen bonding to cytosine H4 and N3 in the ground state, and in addition, donating a proton to N3 to facilitate electron flow onto the departing base in the transition state. Consistent with this mechanism, the nonenzymatic hydrolysis of deoxycytidine is strongly catalyzed by protonation at N3 (pK_a ~4.2) [23].

The present data are not consistent with a previous proposal that Asp123 is anionic [20]. Such a scenario would be strongly anticatalytic through *stabilization* of the neutral ground state by hydrogen bonding, and electrostatic *destabilization* of the negative charge that develops on the base in the transition state [10, 11]. The pH dependence of the residual UDG activity of CYDG declines by 10-fold between pH 6.3 and 8.0 (not shown), which parallels the behavior shown in Figure 2C for the C/Y substrate, and demonstrates that a protonated group with an apparent pK_a in the range ~6–7 is essential for both the C/Y and U/Y glycosylase activities of CYDG. As mentioned earlier, wtUDG and the N123G mutant both show flat pH-rate profiles between pH 7 and 10, providing strong evidence that the essential protonated group is Asp123 [21]. As shown in Figure 5B, a simple protonic tautomerization reaction of Asp123 offers a reasonable explanation for the similar pH dependences of the residual UDG activity of CYDG, and its C/Y glycosylase activity.

Significance

A general and novel approach has been described that allows the isolation and detailed study of UDG mutants that are toxic to bacterial cells. In addition, the substrate rescue method employing the pyrene wedge provides a straightforward strategy to generate DNA glycosylases that are highly specific for N/Y base pairs (where N is the cognate base). We envision that other extremely toxic variants of UDG that would otherwise be lethal to bacterial cells may be expressed using this strategy, and one current goal is to convert UDG into a site-specific RNA glycosidase. We anticipate that this pyrene rescue approach may be used on other glycosidases that do not recognize the base opposite to the cognate damaged base. There is also potential that site-specific DNA glycosylases such as CYDG could be used to quickly and easily detect single nucleotide polymorphisms in genes.

Experimental Procedures

Enzymes

The UDG mutants N123D-L191A and N123G were prepared using the Quick-Change double-stranded mutagenesis kit from Stratagene (La Jolla, CA), and the mutations were confirmed by DNA sequencing of both strands. As previously described, all the enzymes were overexpressed using the pET28a expression vector in BL21(DE3)pLysS and were purified using a Ni-NTA agarose column and streptavidin agarose resin [14, 16].

DNA Substrates

The 11 base pair DNA substrates were synthesized using standard phosphoramidite chemistry with an Applied Biosystems 390 synthesizer as previously described or were obtained from Integrated DNA Technologies (Coralville, IA). The oligonucleotides were purified using anion exchange high-pressure liquid chromatography and desalted using disposable gel filtration columns (PD-10, Amersham Pharmacia Biotech, Piscataway, NJ). The sequences of the duplex DNA molecules are identical except for the target bases in the middle of oligonucleotides (Figure 2A). The 5′-end of the DNA strand-containing target base was labeled with ^{32}P using ^{32}P-γ-ATP (Amersham Pharmacia Biotech, Piscataway, NJ) and T4 polynucleotide kinase (New England BioLabs, Beverly, MA) and the complementary strands were hybridized in buffer A (10 mM NaMES, 25 mM NaCl, and 2.5 mM $MgCl_2$ [pH 6.3] at 25°C).

Enzyme Kinetics

The kinetic measurements were performed in buffer A using CYDG concentrations of 0.25 nM and 50 nM for the U/Y and C/Y substrates. A series of DNA concentrations in the range 15 to 600 nM was used, and the reactions were quenched at times that resulted in less than 20% conversion to product. In all cases, linear initial velocities were observed. At the completion of the measurements, an equal volume of 2 M piperidine was added to quench the reactions, and the samples were heated at 90°C for 20 min to cleave the phosphodiester backbone. The reaction mixtures were lyophilized to dryness and then resuspended in 8 μl of formamide gel loading buffer. The 6-mer products and the 11-mer substrates were resolved on a 20% denaturing polyacrylamide gel. The gels were exposed to a phosphorimaging screen, scanned, and visualized using a BAS 1000 imaging system (FUJIX). The intensities of the bands were quantified using the software Image Reader v1.7E. The concentration of product at each time point was calculated from the intensity ratio [6 mer cpm]/[total cpm] × [total DNA]. The wild-type enzyme, N123G, and N123D-L191A were examined using 11-mer duplex DNA substrates containing C/Y, C/G, U/Y, U/A, T/Y, A/Y, and G/Y base pairs. The observed rate constants (k_{obsd}) were obtained from equation 1.

$$k_{obsd} = \frac{[\text{Product}]}{\text{time} \times [\text{Enzyme}]} \quad (1)$$

The steady-state kinetic parameters were obtained from a plot of k_{obsd} against substrate concentration using equation 2. This form of the Michaelis-Menten equation is valid when the enzyme concentration approaches that of the substrate.

$$k_{obsd} = k_{cat} \times \frac{(b - \sqrt{b^2 - 4[E][S]}}{2[E]}$$

$$b = [E] + [S] + K_m \quad (2)$$

pH Dependence of Cytosine Excision

Four DNA substrates (U/A, U/Y, C/G, and C/Y) were used to access the base excision activity of wtUDG and the N123D:L191A mutant

at different pH values. The reactions were performed by incubation of 250 nM DNA substrate and 100 nM of N123D-L191A (or 10 nM of wtUDG) at 25°C for 30 min (10 min for wtUDG). The observed rate constants were obtained as described above. The data were fitted to equation 3 to obtain the apparent K_{a1} and K_{a2} values for the ascending and descending limbs of the bell-shaped pH dependence of the rates. In equation 3, k_{max} is the maximal rate at the optimal pH, and K_{a1} and K_{a2} are the acid dissociation constants for the acidic and basic limbs of the pH profile.

$$V = \frac{V_{max}}{1 + \frac{[H^+]}{K_{es_1}} + \frac{K_{es_2}}{[H^+]}} \quad (3)$$

DNA Binding Studies of CYDG

The equilibrium dissociation constant for binding the 11-mer duplex DNA substrate containing a C/Y base pair was determined by following the increase in pyrene fluorescence. The sample was excited at 350 nm and the increase of pyrene fluorescence was monitored at 380 nm. The fluorescence intensity was monitored 60 s after mixing the enzyme with a constant concentration of DNA. In this time frame, less than 0.2% of the substrate was cleaved, thereby allowing the measurement of a true dissociation constant. The K_D value was obtained by curve fitting to equation 4, where F_o and F_f are the initial and final fluorescence intensities, respectively.

$$F = F_o - \{(F_o - F_f)[DNA]_{tot}/2\}\{b - (b^2 - 4[E]_{tot}[DNA]_{tot})^{1/2}\}$$

$$b = K_D + [E]_{tot} + [DNA]_{tot} \quad (4)$$

Acknowledgments

We thank members of the Stivers laboratory for reading the manuscript and for their helpful suggestions. This work was supported by National Institutes of Health Grant GM46835.

Received: February 26, 2003
Accepted: March 26, 2003
Published: April 21, 2003

References

1. David, S.S., and Williams, S.D. (1998). Chemistry of glycosylases and endonucleases involved in base-excision repair. Chem. Rev. *98*, 1221–1261.
2. Lindahl, T., and Nyberg, B. (1974). Heat-induced deamination of cytosine residues in deoxyribonucleic acid. Biochemistry *13*, 3405–3410.
3. Pourquier, P., Ueng, L.M., Kohlhagen, G., Mazumder, A., Gupta, M., Kohn, K.W., and Pommier, Y. (1997). Effects of uracil incorporation, DNA mismatches, and abasic sites on cleavage and religation activities of mammalian topoisomerase I. J. Biol. Chem. *272*, 7792–7796.
4. Pogribny, I.P., Muskhelishvili, L., Miller, B.J., and James, S.J. (1997). Presence and consequence of uracil in preneoplastic DNA from folate/methyl-deficient rats. Carcinogenesis *18*, 2071–2076.
5. Stivers, J.T., and Drohat, A.C. (2001). Uracil DNA glycosylase: insights from a master catalyst. Arch. Biochem. Biophys. *396*, 1–9.
6. Atamna, H., Cheung, I., and Ames, B.N. (2000). A method for detecting abasic sites in living cells: age-dependent changes in base excision repair. Proc. Natl. Acad. Sci. USA *97*, 686–691.
7. Stivers, J.T., Pankiewicz, K.W., and Watanabe, K.A. (1999). Kinetic mechanism of damage site recognition and uracil flipping by Escherichia coli uracil DNA glycosylase. Biochemistry *38*, 952–963.
8. Kavli, B., Slupphaug, G., Mol, C.D., Arvai, A.S., Peterson, S.B., Tainer, J.A., and Krokan, H.E. (1996). Excision of cytosine and thymine from DNA by mutants of human uracil-DNA glycosylase. EMBO J. *15*, 3442–3447.
9. Parikh, S.S., Mol, C.D., Slupphaug, G., Bharati, S., Krokan, H.E., and Tainer, J.A. (1998). Base excision repair initiation revealed by crystal structures and binding kinetics of human uracil-DNA glycosylase with DNA. EMBO J. *17*, 5214–5226.
10. Drohat, A.C., and Stivers, J.T. (2000). Escherichia coli uracil DNA glycosylase: NMR characterization of the short hydrogen bond from his187 to uracil O2. Biochemistry *39*, 11865–11875.
11. Drohat, A.C., and Stivers, J.T. (2000). NMR evidence for an unusually low N1 pKa for uracil bound to uracil DNA glycosylase: implications for catalysis. J. Am. Chem. Soc. *122*, 1840–1841.
12. Drohat, A.C., Xiao, G., Tordova, M., Jagadeesh, J., Pankiewicz, K.W., Watanabe, K.A., Gilliland, G.L., and Stivers, J.T. (1999). Hetronuclear NMR and crystallographic studies of wild-type and H187Q Escherichia coli uracil DNA glycosylase: electrophilic catalysis of uracil expulsion by a neutral histidine 187. Biochemistry *38*, 11876–11886.
13. Xiao, G., Tordova, M., Jagadeesh, J., Drohat, A.C., Stivers, J.T., and Gilliland, G.L. (1999). Crystal structure of Escherichia coli uracil DNA glycosylase and its complexes with uracil and glycerol: structure and glycosylase mechanism revisited. Proteins *35*, 13–24.
14. Jiang, Y.L., Song, F., and Stivers, J.T. (2002). Base flipping mutations of uracil DNA glycosylase: substrate rescue using a pyrene nucleotide wedge. Biochemistry *41*, 11248–11254.
15. Jiang, Y.L., and Stivers, J.T. (2002). Mutational analysis of the base flipping mechanism of uracil DNA glycosylase. Biochemistry *41*, 11236–11247.
16. Werner, R.M., Jiang, Y.L., Gordley, R.G., Jagadeesh, G.J., Ladner, J.E., Xiao, G., Tordova, M., Gilliland, G.L., and Stivers, J.T. (2000). Stressing-out DNA? The contribution of serine-phosphodiester interactions in catalysis by uracil DNA glycosylase. Biochemistry *39*, 12585–12594.
17. Kubareva, E.A., Volkov, E.M., Vinogradova, N.L., Kanevsky, I.A., Oretskaya, T.S., Kuznetsova, S.A., Brevnov, M.G., Gromova, E.S., Nevinsky, G.A., and Shabarova, Z.A. (1995). Modified substrates as probes for studying uracil-DNA glycosylase. Gene *157*, 167–171.
18. Parikh, S.S., Walcher, G., Jones, G.D., Slupphaug, G., Krokan, H.E., Blackburn, G.M., and Tainer, J.A. (2000). Uracil-DNA glycosylase-DNA substrate and product structures: conformational strain promotes catalytic efficiency by coupled stereoelectronic effects. Proc. Natl. Acad. Sci. USA *97*, 5083–5088.
19. Jiang, Y.L., Kwon, K., and Stivers, J.T. (2001). Turning on uracil-DNA glycosylase using a pyrene nucleotide switch. J. Biol. Chem. *276*, 42347–42354.
20. Handa, P., Acharya, N., and Varshney, U. (2002). Effects of mutations at tyrosine 66 and asparagine 123 in the active site pocket of Escherichia coli uracil DNA glycosylase on uracil excision from synthetic DNA oligomers: evidence for the occurrence of long-range interactions between the enzyme and substrate. Nucleic Acids Res. *30*, 3086–3095.
21. Drohat, A.C., Jagadeesh, J., Ferguson, E., and Stivers, J.T. (1999). Role of electrophilic and general base catalysis in the mechanism of Escherichia coli uracil DNA glycosylase. Biochemistry *38*, 11866–11875.
22. Segel, I.H. (1993). Enzyme Kinetics. (New York: John Wiley and Sons), pp. 884–942.
23. Shapiro, R., and Danzig, M. (1972). Acidic hydrolysis of deoxycytidine and deoxyuridine derivatives. The general mechanism of deoxyribonucleoside hydrolysis. Biochemistry *11*, 23–29.
24. Waters, T.R., and Swann, P.F. (1998). Kinetics of the action of thymine DNA glycosylase. J. Biol. Chem. *273*, 20007–20014.
25. Shapiro, R., and Kang, S. (1969). Uncatalyzed hydrolysis of deoxyuridine, thymidine, and 5-bromodeoxyuridine. Biochemistry *8*, 1806–1810.
26. Abner, C.W., Lau, A.Y., Ellenberger, T., and Bloom, L.B. (2001). Base excision and DNA binding activities of human alkyladenine DNA glycosylase are sensitive to the base paired with a lesion. J. Biol. Chem. *276*, 13379–13387.
27. Zoltewicz, J.A., Clark, D.F., Sharpless, T.W., and Grahe, G. (1970). Kinetics and mechanism of the acid-catalyzed hydrolysis of some purine nucleosides. J. Amer. Chem. Soc. *92*, pp. 1741–1750.
28. Drohat, A.C., Jagadeesh, J., Ferguson, E., and Stivers, J.T. (1999). The role of electrophilic and base catalysis in the mecha-

nism of Escherichia coli uracil DNA glycosylase. Biochemistry *38*, 11866–11875.
29. Jiang, Y.L., Drohat, A.C., Ichikawa, Y., and Stivers, J.T. (2002). Inhibition of uracil DNA glycosylase by an oxacarbenium ion mimic. Biochemistry *41*, 7116–7124.
30. Jiang, Y.L., Drohat, A.C., Ichikawa, Y., and Stivers, J.T. (2002). Probing the limits of electrostatic catalysis by uracil DNA glycosylase using transition-state mimicry and mutagenesis. J. Biol. Chem. *277*, 15385–15392.
31. Werner, R.M., and Stivers, J.T. (2000). Kinetic isotope effect studies of the reaction catalyzed by uracil DNA glycosylase: evidence for an oxocarbonium ion-uracil anion intermediate. Biochemistry *39*, 14054–14064.